

Distorted Equatorial Coordination Environments and Weakening of U=O Bonds in Uranyl Complexes Containing NCN and NPN Ligands

Mark J. Sarsfield,^{*,†} Madeleine Helliwell,[‡] and James Raftery[†]

Centre for Radiochemistry Research, Department of Chemistry, The University of Manchester, Manchester M13 9PL, United Kingdom

Received November 21, 2003

Treatment of $[\text{UO}_2\text{Cl}_2(\text{thf})_3]$ in thf with 2 equiv of $\text{Na}[\text{PhC}(\text{NSiMe}_3)_2]$ ($\text{Na}[\text{NCN}]$) or $\text{Na}[\text{Ph}_2\text{P}(\text{NSiMe}_3)_2]$ ($\text{Na}[\text{NPN}]$) gives uranyl complex $[\text{UO}_2(\text{NCN})_2(\text{thf})]$ (**1**) or $[\text{UO}_2(\text{NPN})_2]$ (**3**), respectively. Each complex is a rare example of out-of-plane equatorial nitrogen ligand coordination; the latter contains a significantly bent $\text{O}=\text{U}=\text{O}$ unit and represents the first example of a uranyl ion within a quadrilateral-faced monocapped trigonal prismatic geometry. Removal of the thf in **1** gives $[\text{UO}_2(\text{NCN})_2]$ (**2**) with in-plane N donor ligands. Addition of 3 equiv of $\text{Na}[\text{NCN}]$ gives the tris complex $[\text{Na}(\text{thf})_2\text{PhCN}][[\text{UO}_2(\text{NCN})_3]$ (**4**·PhCN) with elongation and weakening of one U=O bond through coordination to Na^+ . Hydrolysis of **4** provides the oxo-bridged dimer $[\text{Na}(\text{thf})\text{UO}_2(\text{NCN})_2]_2(\mu_2\text{-O})$ (**6**), a complex with the lowest reported $\text{O}=\text{U}=\text{O}$ symmetrical stretching frequency ($\nu_1 = 757 \text{ cm}^{-1}$) for a dinuclear uranyl complex. The anion in complex **4** is unstable in solution but can be stabilized by the introduction of 18-crown-6 to give $[\text{Na}(18\text{-crown-6})][[\text{UO}_2(\text{NCN})_3]$ (**5**). The structures of **1–4** and **6** have been determined by crystallography, and all except **2** show significant deviations of the N ligand atoms from the equatorial plane, driven by the steric bulk of the NCN and NPN ligands. Despite the unusual geometries, these distortions in structure do not appear to have any direct effect on the bonding and electronic structure of the uranyl ion. The main influences toward lowering the U=O bond stretching frequency (ν_1) are the donating ability of the equatorial ligands, overall charge of the complex, and $\text{U}=\text{O}\cdots\text{Na}$ -type interactions. The intense orange/red colors of these compounds are because of low-energy ligand-to-metal charge-transfer electronic transitions.

Introduction

From uranium to americium, the actinide metals in the V/VI oxidation states commonly exist as the linear actinyl ion $[\text{AnO}_2]^{x+}$ ($x = 1, 2$), with the uranyl ion $[\text{UO}_2]^{2+}$ being most stable. Typical complexes containing the uranyl unit adopt geometries with the uranyl oxo ligands occupying the axial positions of bipyramidal structures.^{1,2} The limited information from general inorganic textbooks describes the short U=O bonds as inert and indicates that, as a rule, all ancillary ligands are situated in an equatorial plane perpendicular to the $\text{O}=\text{U}=\text{O}$ axis in tetragonal-, pentagonal-, and hexagonal-bipyramidal geometries. Entries into the nonaque-

ous chemistry of the uranyl ion, via $[\text{UO}_2\text{Cl}_2(\text{thf})_3]^3$ and $[\text{UO}_2(\text{OTf})_2]$ ($\text{OTf} = \text{O}_3\text{SCF}_3$),⁴ have unveiled some interesting new discoveries. These include coordination numbers of 3 in the equatorial plane in $[\text{Na}(\text{thf})_2][\text{UO}_2\{\text{N}(\text{SiMe}_3)_2\}_3]^5$ and some uranyl calixarene complexes,^{6,7} the first crystallographically characterized uranyl(V) complex $[\text{UO}_2(\text{Ph}_3\text{PO})_4][\text{O}_3\text{SCF}_3]$,⁸ and the first examples of uranyl–carbon bonds in $[\text{UO}_2\text{Cl}_2(\text{IMes})_2]$ ($\text{IMes} = 1,3\text{-dimesitylimidazol-2-ylidene}$ or $1,3\text{-dimesityl-4,5-dichloroimidazol-2-ylidene}$)⁹ and in

* Author to whom correspondence should be addressed. Fax: +44 (0)-161 275 4616. Phone: +44 (0)161 275 1405. E-mail: mark.j.sarsfield@man.ac.uk

[†] Centre for Radiochemistry Research, Department of Chemistry.

[‡] Department of Chemistry.

(1) Bagnall, K. W. *Comprehensive Coordination Chemistry*; Pergamon: Oxford, 1987; Vol. 3, p 1187.

(2) Katz, J. J.; Morss, L. R.; Seaborg, G. T. *The Chemistry of the Actinide Elements*, 2nd ed.; Chapman and Hall: London, 1986; pp 1137–1140.

(3) Wilkerson, M. P.; Burns, C. J.; Paine, R. T.; Scott, B. L. *Inorg. Chem.* **1999**, *38*, 4156.

(4) Berthet, J. C.; Lance, M.; Nierlich, M.; Ephritikhine, M. *Eur. J. Inorg. Chem.* **2000**, 1969.

(5) Burns, C. J.; Clark, D. L.; Donohoe, R. J.; Duval, P. B.; Scott, B. L.; Tait, C. D. *Inorg. Chem.* **2000**, *39*, 5464–5468.

(6) Thuéry, P.; Nierlich, M.; Masci, B.; Asfari, Z.; Vicens, J. *J. Chem. Soc., Dalton Trans.* **1999**, 3151.

(7) Masci, B.; Nierlich, M.; Thuéry, P. *New J. Chem.* **2002**, *26*, 120.

(8) Berthet, J.-C.; Nierlich, M.; Ephritikhine, M. *Angew. Chem., Int. Ed.* **2003**, *115*, 1996.

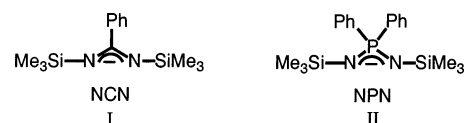
(9) Oldham, W. J.; Oldham, S. M.; Scott, B. L.; Abney, K. D.; Smith, W. H.; Costa, D. A. *Chem. Commun.* **2001**, 1348.

[UO₂Cl{CH(Ph₂PNSiMe₃)₂}thf].^{10,11} Previously assumed to be inert, the U=O ligands continue to display some interesting chemistry with reports of oxo ligand substitution,^{12,13} ligand scrambling between U=O bonds and hydroxides¹⁴ or alkoxides,^{15,16} and the isolation of discrete uranyl compounds exhibiting Lewis basic properties, for example, oxo ligands bridging uranyl centers^{16–19} and coordinating to alkali-metal cations,^{5,16,20} ammonium ions,¹⁴ or strong Lewis acids such as B(C₆F₅)₃.²¹ There are also a growing number of complexes containing non-oxygen-based equatorial ligands that deviate significantly out of the equatorial plane.^{10,11,22–29}

This last point appears to be more common in structurally characterized uranyl compounds than textbooks might suggest. Studies by Alcock et al. on the system [AnO₂(O₂CMe)₂-(bipy)] (An = U, Np)²⁹ and Deacon on [UO₂(O₂C(C₆F₅))₂-(bipy)]²² reported severe ligand distortions from the equatorial plane that can be explained solely on the basis of steric and electrostatic factors and described the “distortability” of the ligands in the order U=O_{axial} < U–O_{equatorial} < U–N_{equatorial}.²⁹ This distortability of the nitrogen ligands is exemplified by the recent report of rhombohedral uranium-centered geometries in [UO₂(OTf)₂(bpy)₂] and [UO₂(phen)₃][OTf]₂.³⁰ Most cases of significant distortions occur in uranyl compounds with chelating ligands in a 6-coordinate equatorial plane.^{24–31} We have demonstrated that, given the correct steric constraints, out-of-plane coordination can be enforced within uranyl complexes with lower coordination numbers. For example, the tridentate ligand [CH(Ph₂PNSiMe₃)₂][–], which disfavors a planar conformation,³² reacts with [UO₂Cl₂(thf)₃]

to give [UO₂Cl{CH(Ph₂PNSiMe₃)₂}thf] containing an out-of-plane U–C bond.^{10,11} This red complex exhibits unusual electronic absorption features that may be a consequence of out-of-plane equatorial coordination. To test this hypothesis, we have synthesized and structurally characterized a number of compounds with severe out-of-plane equatorial distortions to examine how this might affect the bonding in, and electronic absorption characteristics of, the uranyl ion.

Here we explore how the bidentate ligands NCN (**I**) and NPN (**II**), with steric bulk located close to the N donor ligand, can force out-of-plane bonding in a systematic series of complexes with 4–6 equatorial coordination numbers. We examine the effect that this has on the UO₂²⁺ unit, i.e., bond lengths, geometry, vibrational and electronic spectroscopy, and Lewis basic behavior.



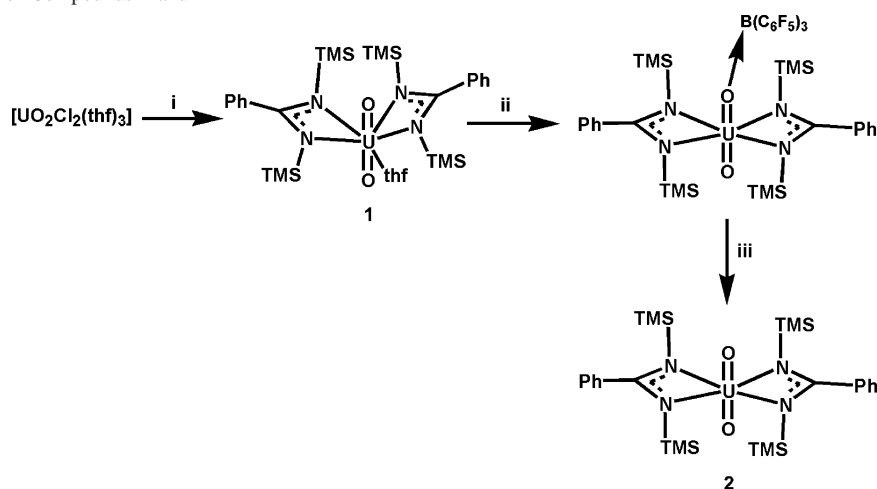
Results and Discussion

Synthesis. Simple metathesis reactions with [UO₂Cl₂(thf)₃] and 2 equiv of Na[NCN] (Na[**I**]) or Na[NPN] (Na[**II**]) in thf gives [UO₂(NCN)₂(thf)] (**1**) or [UO₂(NPN)₂] (**3**), respectively, as an orange solid. Compound **1** has been reported as part of a preliminary investigation, and a brief discussion of the crystallographic data was presented.^{21,33} The thf ligand in **1** coordinates reversibly when dissolved in hydrocarbon solvents. Variable-temperature NMR studies show two exchange processes in solution. One process exchanges the OCH₂ protons that are magnetically inequivalent at –60 °C. The other mechanism involves the exchange of free and coordinated thf. At –60 °C, in the region of slow exchange, the ratio of free to bonded thf is ~6.5:100; thus, most of the thf remains coordinated in solution with a small amount of [UO₂(NCN)₂] (**2**) and free thf present (see the Supporting Information). This is also observed in the solution Raman spectrum of **1** with O=U=O symmetric stretch signals at 803 and 818 cm^{–1} for **1** and **2**, respectively (see the Supporting Information). The coordinated thf in **1** can be removed by using a combination of 2 equiv of B(C₆F₅)₃ followed by 1 equiv of PMe₃ to give **2** (Scheme 1).²¹

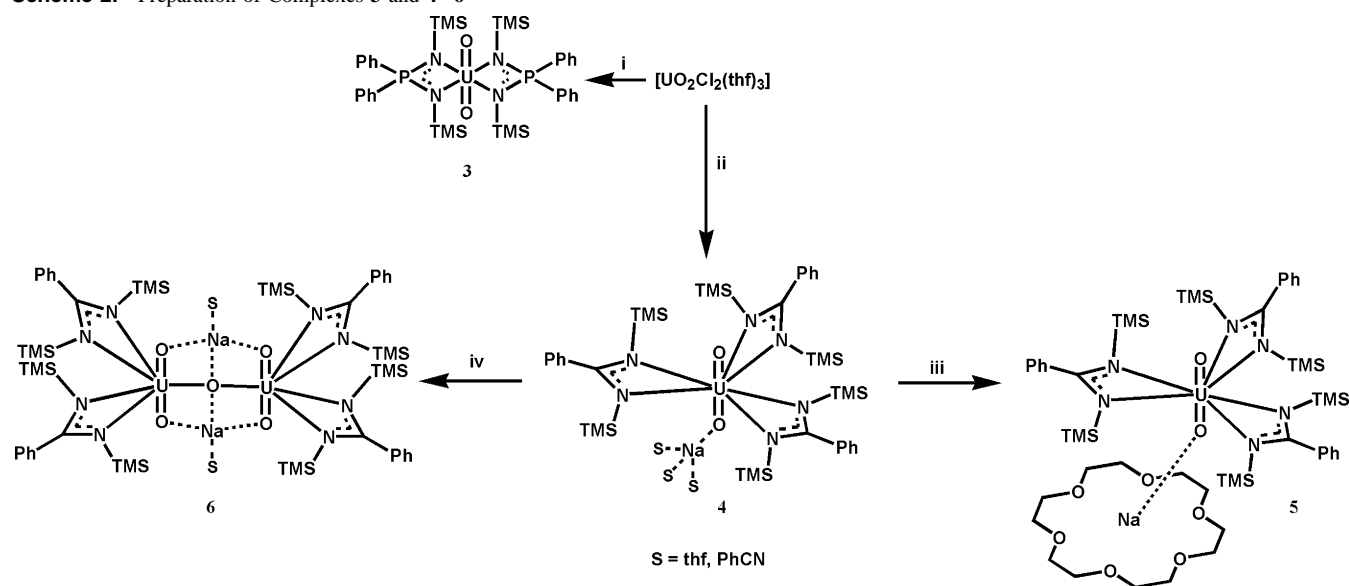
Adding 3 equiv of Na[NCN] to UO₂Cl₂(thf)₃ gives the sodium salt of the tris complex [Na(thf)₂][UO₂(NCN)₃]·¹/₂PhCN (**4**·¹/₂PhCN) in the crystalline form, but elemental analysis (C, H, N, U, Na), after the powdery orange solid is dried in vacuo, gives satisfactory matches for the molecular formula [Na(thf)₂][UO₂(NCN)₃] (**4**). In solution, the analysis

- (10) Sarsfield, M. J.; Helliwell, M.; Collison, D. *Chem. Commun.* **2002**, 2264.
 (11) Sarsfield, M. J.; Helliwell, M.; Steele, H.; Tate, S. *J. Chem. Soc., Dalton Trans.* **2003**, 3443.
 (12) Brown, D. R.; Denning, R. G. *Inorg. Chem.* **1996**, *35*, 6158.
 (13) Williams, V. C.; Müller, M.; Leech, M. A.; Denning, R. G.; Green, M. L. H. *Inorg. Chem.* **2000**, *39*, 2538.
 (14) Clark, D. L.; Conradson, S. D.; Donohoe, R. J.; Keogh, D. W.; Morris, D. E.; Palmer, P. D.; Rogers, R. D.; Tait, C. D. *Inorg. Chem.* **1999**, *38*, 1456–1466.
 (15) Burns, C. J.; Sattelberger, A. P. *Inorg. Chem.* **1988**, *27*, 3692–3693.
 (16) Wilkerson, M. P.; Burns, C. J.; Dewey, H. J.; Martin, J. M.; Morris, D. E.; Paine, R. T.; Scott, B. L. *Inorg. Chem.* **2000**, *39*, 5277.
 (17) Burns, C. J.; Sattelberger, A. P. *Inorg. Chem.* **1988**, *27*, 3692.
 (18) Taylor, J. C.; Ekstrom, A.; Randall, C. H. *Inorg. Chem.* **1978**, *17*, 3285.
 (19) Thuéry, P.; Nierlich, M.; Souley, B.; Asfari, Z.; Vincens, J. *J. Chem. Soc., Dalton Trans.* **1999**, 2589.
 (20) Danis, J. A.; Lin, M. R.; Scott, B. L.; Eichhorn, B. W.; Runde, W. H. *Inorg. Chem.* **2001**, *40*, 3389.
 (21) Sarsfield, M. J.; Helliwell, M. *J. Am. Chem. Soc.* **2004**, *126*, 1036.
 (22) Deacon, G. B.; Makinnon, P. I.; Taylor, J. C. *Polyhedron* **1985**, *4*, 103.
 (23) Sitran, S.; Fregona, D.; Casellato, U.; Vigato, P. A.; Graziani, R.; Faraglia, G. *Inorg. Chim. Acta* **1987**, *132*, 279.
 (24) Sessler, J. L.; Seidel, D.; Vivian, A. E.; Lynch, V.; Scott, B. L.; Keogh, W. *Angew. Chem., Int. Ed.* **2001**, *40*, 591.
 (25) Paoletti, G.; Marangoni, G.; Bandoli, G.; Clemente, D. A. *J. Chem. Soc., Dalton Trans.* **1979**, 459.
 (26) Navaza, A.; Villain, F.; Charpin, P. *Polyhedron* **1984**, *3*, 143.
 (27) Jayadevan, N. C.; Mudher, K. D. S.; Chackrabarty, D. M. *Acta Crystallogr., Sect. B: Struct. Sci.* **1975**, *31*, 2277.
 (28) Alcock, N. W.; Flanders, D. J.; Pennington, M.; Brown, D. *Acta Crystallogr., Sect. C: Cryst. Struct. Commun.* **1988**, *44*, 247.
 (29) Alcock, N. W.; Flanders, D. J.; Pennington, M.; Brown, D. *J. Chem. Soc., Dalton Trans.* **1985**, 1001.
 (30) Berthet, J.-C.; Nierlich, M.; Ephritikhine, M. *Chem. Commun.* **2003**, 1660.
 (31) Sitran, S.; Fregona, D.; Casellato, U.; Vigato, P. A.; Graziani, R.; Faraglia, G. *Inorg. Chim. Acta* **1987**, *132*, 279.

- (32) Babu, R. P. K.; Aparna, K.; McDonald, R.; Cavell, R. G. *Organometallics* **2001**, *20*, 1451–1455.
 (33) Wedler, M.; Roesky, H. W.; Edelmann, F. *J. Organomet. Chem.* **1988**, *345*, C1.
 (34) These data were collected from the Cambridge crystallographic database. From the 587 hits of uranyl structures with RFAC < 10%, the mean U=O distance is 1.762 Å with a standard deviation of 0.033 Å. This relates to an approximate range of 1.696–1.828 Å within a 95% confidence limit.
 (35) Allen, F. H.; Davies, J. E.; Galloy, J. J.; Johnson, O.; Kennard, O.; Macrae, C. F.; Mitchell, E. M.; Mitchell, G. F.; Smith, J. M.; Watson, D. G. *J. Chem. Inf. Comput. Sci.* **1991**, *31*, 187.

Scheme 1. Preparation of Compounds 1 and 2^a

^a Reagents and conditions: (i) 2Na[NCN]; (ii) 2B(C₆F₅)₃; (iii) PMe₃.

Scheme 2. Preparation of Complexes 3 and 4–6^a

^a Reagents and conditions: (i) 2Na[NPN]; (ii) 3Na[NCN]; (iii) 18-crown-6; (iv) H₂O.

of this compound was inconsistent with the formulation of **4**, with more than one SiMe₃ signal observed in the ¹H and ¹³C NMR spectra. The NMR data are consistent with some of the complex dissociating to give a mixture of Na[NCN], **1**, **4**, and free PhCN. It was considered that the removal of PhCN and possibly thf from the coordination sphere of Na⁺ renders the anion in complex **4** unstable in hydrocarbon solution. The integrity of the anion in **4** improved considerably with the addition of 18-crown-6 to form the more stable [Na(18-crown-6)][[UO₂(NCN)₃] (**5**). Fortuitous partial hydrolysis of **4**, during recrystallization, provides the oxo-bridged dimer [Na(thf)UO₂(NCN)₂]₂(μ₂-O) (**6**) in low yield (Scheme 2). Attempts to synthesize **6** by controlled hydrolysis were unsuccessful. The presence of the ligands for all compounds is confirmed in the solid state by Raman spectroscopy and elemental analysis that match expected values (C, H, N, U) for the formulas **1**–**5**. Solutions of **3** show a significant shift in the ³¹P NMR upon complexation of the NPN ligand (δ 14.6 ppm; cf. δ 8.7 ppm for NaNPN). Compounds **1**–**3** and **5** show chemical shifts different from

those of free ligand by ¹H and ¹³C NMR spectroscopy and have the same Raman spectrum in solution as in the solid state, evidence to suggest that these compounds remain intact in solution. The difference in geometry and coordination number between **3** and **1** is attributed to the size of the ligand bite angle at the uranium center (NPN, N(1)–U(1)–N(2) = 61.87(13)° (**3**); NCN, N–U–N = 54.87(16)° (**1**)). The smaller bite angle in **1** allows enough room for an additional coordination site to be occupied.

Structures. [UO₂(NCN)₂(thf)] (**1**). A brief description of structure **1** has been reported elsewhere.²¹ The uranium center is 7-coordinate with a thf molecule and two bidentate benzaminato ligands that are twisted out of the equatorial plane by 23.8° and 24.5° (from the plane normal to the vector defined by the uranyl oxygens) corresponding to ligand atom equatorial displacement between 0.14 and 0.62 Å (Table 3). The large distortions suggest that the geometry of the molecule can no longer be described as pentagonal bipyramidal.^{36,37} The uranyl unit is significantly bent (O–U–O = 169.7(2)°) toward the thf ligand. This bend is no doubt due

Table 1. Crystallographic Data for Complexes **2**, **3**, **4** and **6**

	2	3 ^{1/2} toluene	4 ^{1/2} PhCN	6
empirical formula	C ₂₆ H ₄₆ N ₄ O ₂ Si ₄ U	C _{39.50} H ₆₀ N ₄ O ₂ P ₂ Si ₄ U	C _{50.5} H _{87.5} N _{6.5} NaO ₄ Si ₆ U	C ₆₀ H ₁₀₈ N ₈ Na ₂ O ₇ Si ₈ U ₂
mol wt	797.06	1035.24	1279.33	1800.30
cryst syst	monoclinic	monoclinic	monoclinic	monoclinic
<i>a</i> /Å	23.534(9)	16.717(4)	14.344(6)	31.242(9)
<i>b</i> /Å	11.315(4)	13.625(3)	20.471(8)	37.329(9)
<i>c</i> /Å	15.428(6)	21.017(5)	21.209(8)	24.428(6)
α/deg	90	90.0	90	90
β/deg	124.896(5)	93.519(5)	99.386(7)	106.561(6)
γ/deg	90	90.0	90	90
<i>V</i> /Å ³	3370(2)	4778(2)	6144(4)	27307(13)
<i>T</i> /K	100(2)	100(2)	100(2)	100(2)
space group	<i>C</i> 2/ <i>c</i>	<i>P</i> 21/ <i>c</i>	<i>P</i> 21/ <i>n</i>	<i>C</i> 2/ <i>c</i>
<i>Z</i>	4	4	4	12
μ(Mo Kα)/mm ⁻¹	4.987	3.600	2.810	3.711
no. of collected reflns	9461	26579	48267	97541
no. of unique reflns	9461	9808	12567	24490
R1 [<i>I</i> > 2σ(<i>I</i>)]	0.0599	0.0385	0.0439	0.0725
wR2 [<i>I</i> > 2σ(<i>I</i>)]	0.1306	0.0890	0.0616	0.1269

Table 2. Selected Bond Distances and Angles for Complexes **2**, **3**, **4** and **6**

2		3		4		6	
U(1)–O(1)	1.750(4)	U(1)–O(1)	1.784(3)	U(1)–O(1)	1.783(3)	U(1)–O(3)	1.817(12)
U(1)–O(2)	1.750(4)	U(1)–O(2)	1.778(3)	U(1)–O(2)	1.812(3)	U(1)–O(4)	1.828(12)
U(1)–N(1)	2.408(5)	U(1)–N(1)	2.460(4)	U(1)–N(1)	2.521(4)	U(2)–O(1)	1.819(13)
U(1)–N(2)	2.429(5)	U(1)–N(2)	2.492(4)	U(1)–N(2)	2.523(4)	U(2)–O(2)	1.795(12)
U(1)–N(3)	2.408(5)	U(1)–N(3)	2.437(4)	U(1)–N(3)	2.570(5)	U(2)–N(1)	2.439(15)
U(1)–N(4)	2.429(5)	U(1)–N(4)	2.480(4)	U(1)–N(4)	2.489(9)	U(1)–N(5)	2.491(13)
				U(1)–N(5)	2.571(4)	U(2)–O(5)	2.220(13)
				U(1)–N(6)	2.542(7)	U(1)–O(5)	2.180(13)
				Na(1)–O(2)	2.204(4)	Na(1)–O(2)	2.252(13)
						Na(1)–O(5)	2.477(15)
O(1)–U(1)–O(2)	179.4(3)	O(2)–U(1)–O(1)	177.5(2)	O(1)–U(1)–O(2)	178.6(2)	O(2)–U(2)–O(1)	174.3(5)
N(1)–U(1)–N(2)	56.1(2)	N(1)–U(1)–N(2)	61.9(1)	N(1)–U(1)–N(2)	53.6(1)	N(2)–U(2)–N(1)	56.1(5)
N(1)–C(1)–N(2)	120.0(6)	N(2)–P(1)–N(1)	104.9(2)	N(1)–C(1)–N(2)	117.7(4)	N(2)–C(1)–N(1)	113.0(18)
N(1)–U(1)–N(1A)	175.9(2)					O(1)–U(2)–O(5)	87.8(5)
						U(1)–O(5)–U(2)	171.6(5)

Table 3. Deviations of Ligand Atoms, within the Inner Coordination Sphere, from the Theoretical Equatorial Plane (Å)^a

3		2		4		6	
						For U1	
N1	0.103	N1	0.338	N1	–0.540	N1	–0.370
N2	–0.070	N2	–0.290	N2	0.520	N2	0.548
N1A	–0.103	N3	0.233	N3	–0.595	N3	–0.718
N2A	0.070	N4	–0.342	N4	0.417	N4	0.446
C1	0.032	P1	0.073	N5	–0.610	O5	–0.020
C1A	–0.032	P2	–0.115	N6	0.590	C1	0.197
				C1	–0.027	C14	–0.282
				C14	–0.138	For U2	
				C27	–0.007	N5	–0.502
						N6	0.291
						N7	–0.516
						N8	0.743
						O5	0.050
						C27	–0.225
						C40	0.169

^a The theoretical equatorial plane is defined by the plane, normal to the line defined by the oxo ligands, that passes through the uranium atom.

to the close contacts between the NCN ligand and oxo ligands (Table 4). Two of the nitrogen ligand atoms are situated nearly trans to each other (N–U–N = 177.09(16)°). The overall 7-coordinate geometry can be visualized as a trigonal prism that is capped by the thf oxygen atom on a

(36) Drew, M. G. B. *Prog. Inorg. Chem.* **1977**, *23*, 67.

(37) Howard, J. A. K.; Copley, R. C. B.; Yao, J. W.; Allen, F. H. *Chem. Commun.* **1998**, 2175.

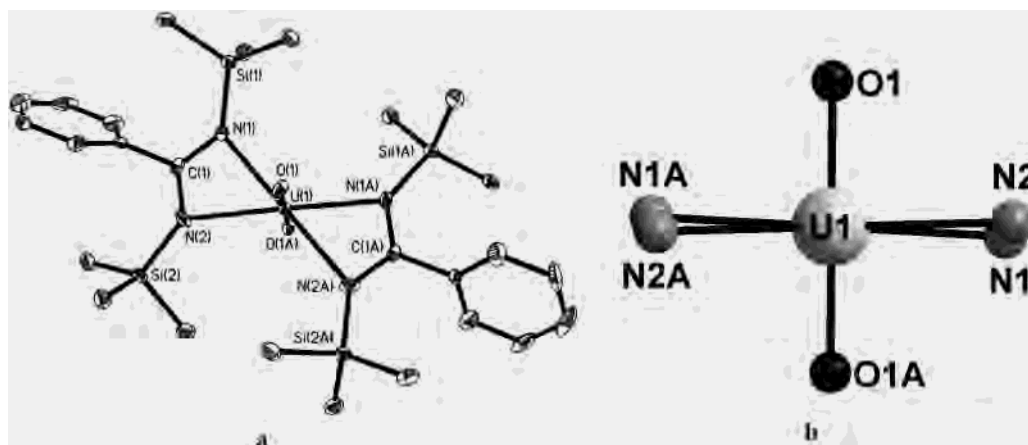
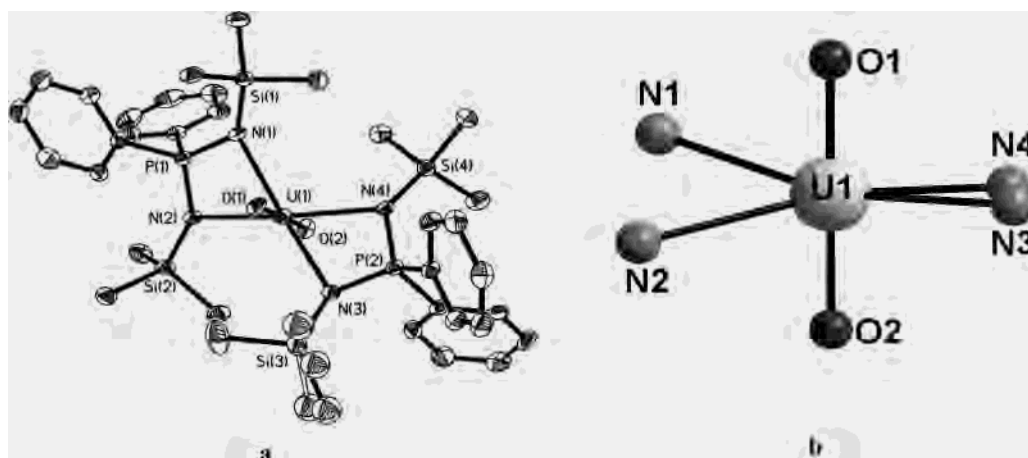
quadrilateral face. It is noteworthy that, rather than remain in the equatorial plane, the NCN ligands twist to allow a thf molecule to bond and increase the coordination number to 7. We have found that the reaction between [UO₂Cl₂(thf)₃] and excess amounts of the ligands [X(Ph₂PNSiMe₃)₂][–] (X = CH, N) gave only the monosubstituted [UO₂{X(Ph₂PNSiMe₃)₂}Cl(thf)] or solvent-free dinuclear complexes [UO₂{X(Ph₂PNSiMe₃)₂}Cl]₂.¹¹ All of these compounds have N–U–N bite angles of > 115°.

[UO₂(NCN)₂] (2). The synthesis of **2** has been reported;²¹ however, the crystal structure of this compound was not discussed. Removal of thf from **1** provides an interesting comparison in terms of the steric factors involved in ligand displacement from the equatorial plane. An ORTEP representation of **2** is shown in Figure 1a. The uranium is at the center of a distorted octahedral environment bonded to two NCN ligands together with a linear O=U=O group (179.4(3)°). Compared to **1** and **3**, complex **2** is less crowded, allowing all the ligands to move closer to the uranium center demonstrated by the in-plane nitrogen ligands (Figure 1b and Table 3) and the reduction of the U=O (1.750(4) Å) and U–N bond lengths (U–N_{av} = 2.418(5) Å) (cf. (**3**) U=O = 1.781(3) Å and U–N_{av} = 2.467(4) Å and (**1**) U=O = 1.778(3) Å and U–N_{av} = 2.463(4) Å).²¹

[UO₂(NPN)₂] (3). Single crystals of **3** suitable for X-ray crystallography were grown from toluene solutions. An

Table 4. The Four Closest Contacts between the N and Oxo Ligands (Å) in Complexes 1–4 and 6

	1		2		3		4		6	
N1–O1	2.874(6)	N1–O1	3.040(12)	N1–O1	2.854(5)	N1–O2	2.790(9)	N1–O2	2.783(20)	
N2–O2	2.765(6)	N2–O1	2.949(12)	N2–O2	2.877(6)	N2–O1	2.785(9)	N2–O1	2.741(24)	
N3–O1	2.926(6)	N1A–O1	2.919(9)	N3–O1	2.861(5)	N3–O2	2.768(6)	N3–O2	2.713(21)	
N4–O1	2.789(6)	N2A–O1	3.031(9)	N4–O2	2.861(5)	N4–O1	2.789(9)	N4–O1	2.866(25)	
	2.838		2.985	av	2.863		2.783		2.777	

**Figure 1.** (a) Molecular structure and atom labeling scheme for **2** with H atoms omitted (50% probability ellipsoids). (b) Ball-and-stick representation illustrating the in-plane bonding showing only the atoms coordinated directly to uranium for clarity.**Figure 2.** (a) Molecular structure and atom labeling scheme for **3** with H atoms omitted (50% probability ellipsoids). (b) Ball-and-stick representation illustrating the out-of-plane bonding showing only the atoms coordinated directly to uranium for clarity.

ORTEP representation of **3** is shown in Figure 2. The asymmetric unit contains one molecule, together with $1/2$ a toluene molecule, the latter being disordered. The uranyl ion has typical U=O bond lengths (U(1)–O(1) = 1.784(3) Å),^{34,35} and the O=U=O angle ((O(1)–U(1)–O(2) = 177.54(15)°) is near linear and in the range for other structurally characterized uranyl complexes (98% of the structures have O=U=O angles that lie within 180–174°).³⁵ The uranium is coordinated to two bidentate diiminophosphinate ligands that are equally twisted out of the equatorial plane in a distorted octahedral geometry. The two planes defined by N1, P1, N2 and N3, P2, N4 are at angles of $\sim 14.6^\circ$ and $\sim 13.5^\circ$, respectively, to the plane normal to the vector defined by the uranyl oxo ligands (the hypothetical equatorial plane). This can be visualized in Figure 2b where the molecule is oriented such that one of the ligands appears in the plane while the other is displaced from it. The U–N bonds (2.437(4)–2.491(4) Å) are somewhat shorter than

neutral N donor U–N bonds (e.g., [UO₂(OTf)₂(py)₃], 2.541(2)–2.518(2) Å)⁴ and those reported for [UO₂{X(Ph₂PNSiMe₃)₂}Cl] (X = CH, N; U–N = 2.510(3)–2.593(11) Å),^{10,11} but are longer than the U–N bonds in [Na(thf)₂][UO₂{N–(SiMe₃)₂}₃] (2.310(4) Å).⁵

[Na(thf)₂(PhCN)_{0.5}][UO₂(NCN)₃] (**4**– $1/2$ PhCN). The structure of complex **4** is shown in Figure 3 as an ORTEP diagram with SiMe₃ groups and disordered thf and PhCN molecules, coordinated to the sodium ion, omitted for clarity. Three bidentate benzaminate ligands are arranged in a propeller-like structure around the nearly linear uranyl ion (O=U=O = 178.55(16)°). Each of the NCN ligands is displaced out of the equatorial plane by 0.42–0.61 Å (Table 3). The U=O bond lengths are unsymmetrical due to the coordination of a sodium ion (O(2)–Na = 2.204(4) Å) to an oxo ligand (U–O(1) = 1.783(3) Å; U–O(2) = 1.812(3) Å). It is interesting to note that, for the related tris(phenylacetate) complex [Na(H₂O)₂][UO₂(PhCO₂)₃], the sodium atom co-

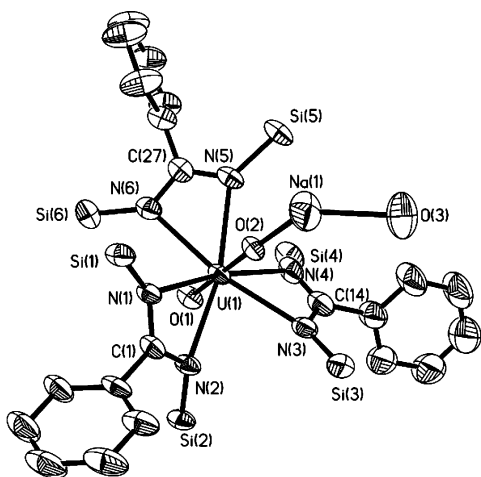


Figure 3. An ORTEP representation with 50% probability ellipsoids of $4 \cdot \frac{1}{2}\text{PhCN}$. The methyl groups on Si atoms and disordered solvent molecules around the sodium atom have been removed for clarity.

ordinates to the equatorial rather than axial oxygens. This difference in cation coordination site could originate from packing forces in the crystal lattice or from the preference of Na^+ to coordinate to the harder O donor over the N donor atoms in **4**. Another explanation is that the electron-donating ability of equatorial ligands influences the Lewis basic properties of the uranyl oxo groups. This phenomenon is observed in a number of uranyl compounds containing strongly basic ligand groups (e.g., $[\text{Na}(\text{thf})_2][\text{UO}_2\{\text{N}(\text{SiMe}_3)_2\}_3]$ ($\text{U}=\text{O} = 1.810(5)$ and $1.781(5)$ Å; $\text{O}-\text{Na} = 2.201(6)$ Å)⁵ and $[\text{Na}(\text{thf})_3]_2[\text{UO}_2(\text{O}-2,6\text{-Me}_2\text{C}_6\text{H}_3)_4]$ ($\text{U}=\text{O} = 1.816(5)$ and $1.812(5)$ Å; $\text{O}-\text{Na} = 2.357(6)$ Å)).³⁸ Compared to the benzoate ligand $[\text{PhCO}_2]^-$, the basicities of the NCN ligands in **4** are probably enhanced by the fact that the Ph group is twisted out of the NCN plane (torsion angle $\text{N}(1)-\text{C}(1)-\text{C}(2)-\text{C}(7) = 68.8(6)^\circ$), preventing conjugation of the negative charge throughout the phenyl ring. In $[\text{Na}(\text{H}_2\text{O})_2][\text{UO}_2(\text{PhCO}_2)_3]$ the Ph groups are coplanar with the carboxylate groups. The equatorial oxygens in $[\text{Na}(\text{H}_2\text{O})_2][\text{UO}_2(\text{PhCO}_2)_3]$ do not deviate from the equatorial plane by more than ± 0.2 Å.³⁹

$[\text{Na}(\text{thf})\text{UO}_2(\text{NCN})_2](\mu\text{-O})$ (6**).** During the recrystallization of **4** from hexane, a second crop of crystals exhibiting a different morphology was isolated. The crystal structure was solved in two different space groups, rhombohedral $R\bar{3}$ and monoclinic $C2/c$, with the latter providing the most satisfactory refinement. The asymmetric unit contains 1.5 molecules of **6**, and an ORTEP representation of one molecule is shown in Figure 4 with all carbon and silicon atoms removed to illustrate clearly the dimetallic core (the whole molecule can be viewed in Scheme 2). The structure consists of two parallel uranyl units, each coordinated to two NCN ligands, and bridged by an oxide group. The bridging oxide is nearly linear ($\text{U}(1)-\text{O}(5)-\text{U}(2) = 171.6(5)^\circ$) and is unlikely to be a bridging hydroxide observed in other

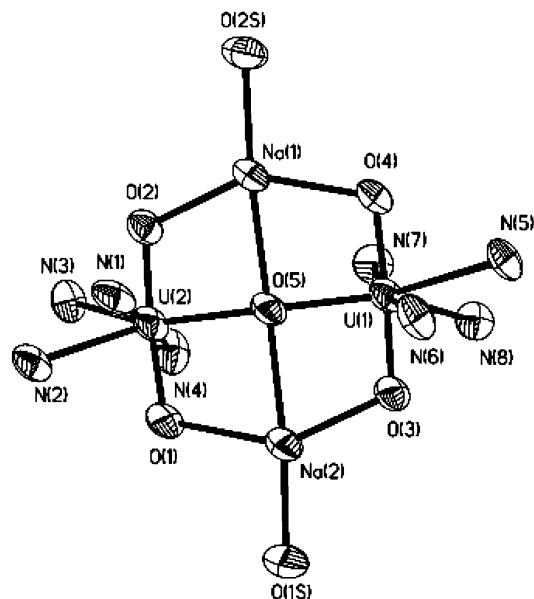


Figure 4. ORTEP representation of **6** with all hydrogen, carbon, and silicon atoms removed to clearly illustrate the dinuclear core.

dinuclear uranyl compounds.^{26,40,41} While $\mu_3\text{-O}$ groups are known in uranyl cluster compounds,^{42,43} to our knowledge, the only other reported $\mu_2\text{-O}$ compound with this structural motif is $[\{\text{UO}_2(\text{py})_4\}_2(\mu_2\text{-O})][\text{OS}(\text{O})_2\text{CF}_3]_2$, which contains uranyl groups oriented perpendicular to each other to reduce electrostatic repulsions.⁴ In **6** the oxo ligands are stabilized in a parallel arrangement with short interatomic contacts to two Na ions (four Na–oxo contacts, ranging from 2.211(15) to 2.303(16) Å) similar to those found in **4**. Each Na ion is coordinated to one thf molecule ($\text{Na}(2)-\text{O}(1\text{S}) = 2.136(17)$ Å; $\text{Na}(1)-\text{O}(2\text{S}) = 2.220(17)$ Å) with a longer contact to the bridging oxide ($\text{Na}(1)-\text{O}(5) = 2.477(15)$; $\text{Na}(2)-\text{O}(5) = 2.498(15)$ Å). The $\text{U}=\text{O}$ bonds ($1.795(12)$ – $1.828(12)$ Å) are lengthened compared to those of **1**, **2**, and $[\{\text{UO}_2(\text{py})_4\}_2(\mu_2\text{-O})][\text{OS}(\text{O})_2\text{CF}_3]_2$ ($\text{U}=\text{O}_{\text{av}} = 1.774(2)$ Å). The short $\text{U}-\mu_2\text{-O}$ bonds ($\text{U}(1)-\text{O}(5) = 2.180(13)$; $\text{U}(2)-\text{O}(5) = 2.220(13)$ Å) are of length comparable to those in $[\{\text{UO}_2(\text{py})_4\}_2(\mu_2\text{-O})][\text{OS}(\text{O})_2\text{CF}_3]_2$ ($\text{U}-\text{O} = 2.105(5)$ and $2.085(5)$ Å).⁴ Once again, the N donor ligands are significantly displaced from the uranyl equatorial plane (0.29 – 0.74 Å) (Table 3), and yet they are slightly closer to the uranium center ($\text{U}-\text{N}_{\text{av}} = 2.506(15)$ Å) than in $[\{\text{UO}_2(\text{py})_4\}_2(\mu_2\text{-O})][\text{OS}(\text{O})_2\text{CF}_3]_2$ ($\text{U}-\text{N}_{\text{av}} = 2.594(5)$ Å), despite the fact that the dinuclear uranium system in the latter has an overall $2+$ charge.⁴

Discussion of Structures 1–4 and 6. All the structures reported here illustrate that by choosing a ligand with large steric bulk it is easy to distort the classical bipyramidal geometries accepted as the normal structural motifs for actinyl complexes. Although slight puckering of 8-coordinate

(38) Barnhart, D. M.; Burns, C. J.; Sauer, N. N.; Watkin, J. G. *Inorg. Chem.* **1995**, *34*, 4079.

(39) Bismondo, A.; Casellato, U.; Graziani, R. *Inorg. Chim. Acta* **1994**, *223*, 151.

(40) Jiang, J.; Sarsfield, M. J.; Renshaw, J. C.; Livens, F. R.; Collison, D.; Charnock, J. M.; Helliwell, M.; Eccles, H. *Inorg. Chem.* **2002**, *41*, 2799.

(41) Viossat, P. B.; Dung, N.; Soye, C. *Acta Crystallogr., Sect. C: Cryst. Struct. Commun.* **1983**, *C39*, 573.

(42) Nierlich, M.; Souley, B.; Asfari, Z.; Vicens, J. *J. Chem. Soc., Dalton Trans.* **1999**, 2589.

(43) Aberg, M. *Acta Chem. Scand.* **1978**, *A32*, 101.

geometries by ± 0.2 Å around the equatorial plane is known, the propeller arrangement of ligands in **4** is far removed from that of a hexagonal-bipyramidal geometry. Metal complexes with high coordination numbers (>7) generally have small energy barriers to distortions in geometry, and yet, in this study, complexes with coordination numbers of 6 (**3**) and 7 (**1** and **6**) show significant deviations from classical bipyramidal geometries. The increase in coordination number and ligand bite angle at the uranium may explain the greater U–N bond lengths in **1** and **3** compared to **2**. We believe that this can also be partly related to the amount of charge donated to the metal center. Our previous studies have shown that, by removing electron density from the uranium center in **2** through one of the axial ligands, by coordinating to a Lewis acid as in $[\text{UO}\{\text{OB}(\text{C}_6\text{F}_5)_3\}(\text{NCN})_2]$ ($U-N_{\text{av}} = 2.371(4)$ Å)²¹ (Scheme 1), the U–N bond lengths decrease (cf. (**2**) $U-N_{\text{av}} = 2.418(5)$ Å). Thus, if you increase charge donation to the uranium, the U–N bonds increase, and this is reflected in the distribution of U–N bond lengths in the series **2–4** (Table 2). It is also reassuring to observe the same trend in ligand distortability as observed by Alcock et al. as expected when using hard/soft ligand donor arguments. For example, distortions of the equatorial nitrogen ligands are greater compared to those of equatorial oxygen-based ligands when **2** is compared to **1** (thf) or **6** (O^-) (Table 3).

Uranyl oxo interactions with cations, as observed in the solid state for **4** and **6**, have been reported in some of the earliest crystal structure determinations of uranates $\text{M}(\text{UO}_2)\text{-O}_2$ [$\text{M} = \text{Mg}, \text{Ca}, \text{Sr}$] containing the uranyl subunit,^{44–46} and the increase in the U=O bond length is related to the decrease in bond strength calculated empirically by valence sum methods.⁴⁴ There is evidence for actinyl–oxygen–metal interaction in neptunyl(V) chemistry, although there are no reports of $\text{NpO}_2^+\cdots\text{Na}^+$ interactions in solution or the solid state. Crystallographic studies do show that $[\text{NpO}_2]^+$ can participate in networks of $\text{NpO}_2^+\cdots\text{NpO}_2^+$ interactions via oxo ligands,^{47–49} and this behavior is also observed in solution with NpO_2^+ coordinating to a number of metal cations ($\text{Rh}^{\text{III}}, \text{Cr}^{\text{III}}, \text{NpO}_2^+, \text{UO}_2^{2+}$).^{50–52} This Lewis basic property of the neptunyl oxygens is attributed to the f^2 electrons centered on neptunium, causing electron density within the $\text{Np}=\text{O}$ bond to be polarized toward oxygen.⁵³ Precedence for this type of behavior in actinyl(VI) compounds is only observed in a number of UO_2^{2+} complexes in the solid state.^{16,18,19,54–58} For example, tetrameric

Table 5. Raman Symmetric Stretching Frequency for the $\text{O}=\text{U}=\text{O}$ Unit in **1–6**

complex	$\nu_1(\text{O}=\text{U}=\text{O})$ (cm^{-1})		complex	$\nu_1(\text{O}=\text{U}=\text{O})$ (cm^{-1})	
	solid	solution		solid	solution
1	803	822, 803	4	773	na
2	818	822	5	785	782
3	824	820	6	757	na

$[\text{UO}_2(\text{OCH}(\text{iPr})_2)_4]$ contains bridging $\text{UO}_2^{2+}\cdots\text{UO}_2^{2+}$ metal–oxo ligand interactions with the coordinating U=O bond elongated ($\text{U}=\text{O} = 1.846(4)$ Å).¹⁶ There is only one report, on solutions of $[\text{UO}\{\text{OB}(\text{C}_6\text{F}_5)_3\}(\text{NCN})_2]$, in which these Lewis basic interactions are shown to exist in solution.²¹ Of course, the origin of this coordination mode differs from that in NpO_2^+ since U(VI) contains no f electrons, but we and others^{16,19,20,57,58} are accumulating evidence consistent with the fact that the loading of charge at the uranium center, by strong electron-donating ligands, causes an increase in oxo ligand basicity, thus allowing $\text{An}=\text{O}\cdots\text{M}$ -type interactions to occur.

Vibrational Spectroscopy. It is well established that strong electron-donating ligands can weaken U=O bonding in the uranyl ion and that Raman spectroscopy is a much more sensitive tool for investigating this than crystallographic studies.^{14,59–61} We recognize that both the symmetric and asymmetric stretches should be considered when commenting on bond strengths.⁶² Unfortunately, the asymmetric stretch (ν_3) was often obscured in the IR spectra of uranyl complexes containing these organic ligands, so for qualitative comparisons, in this family of complexes, only the symmetric $\text{O}=\text{U}=\text{O}$ stretch (ν_1) is discussed. In **1–6**, there is a large decrease in ν_1 (from 829 (**3**) to 757 (**6**) cm^{-1}) compared to that in $[\text{UO}_2\text{Cl}_2(\text{thf})_2]_2$ (834 cm^{-1}) (the solid-state precursor to $[\text{UO}_2\text{Cl}_2(\text{thf})_3]$), which is considered a normal value of ν_1 for weak-field ligands (Table 5). The factors that may contribute to U=O bond weakening are (1) electron-donating ability of the ligand, (2) bending of the $\text{O}=\text{U}=\text{O}$ bonds, (3) out-of-plane equatorial coordination, (4) cation coordination to U=O, (5) coordination number/ligand denticity, and (6) overall charge on the complex. To try to rationalize the main influences on U=O bond weakening, important comparisons can be made among compounds **1–6**. First, we believe that out-of-plane equatorial ligand bonding does not effect the $\text{O}=\text{U}=\text{O}$ symmetric stretch (ν_1) given that distorted **3** (829 cm^{-1}) has a higher ν_1 than **2** (818 cm^{-1}). It is evident that the number of ligands and the charge they donate are the main influences. There is a decrease in the $\text{O}=\text{U}=\text{O}$ symmetric stretch on going from $[\text{UO}_2\text{Cl}_2(\text{thf})_2]_2$ to **3** or **1**

(44) Zachariasen, W. H. *Acta Crystallogr.* **1954**, *7*, 795.

(45) Zachariasen, W. H. *Acta Crystallogr.* **1954**, *7*, 788.

(46) Zachariasen, W. H. *Acta Crystallogr.* **1948**, *1*, 281.

(47) Cousson, P. A. *Acta Crystallogr., Sect. C: Cryst. Struct. Commun.* **1985**, *C41*, 1758.

(48) Cousson, A.; Dabos, S.; Abazil, H.; Nectoux, F.; Pagés, M.; Choppin, G. *J. Less-Common Met.* **1984**, *99*, 233.

(49) Grigor'ev, M. S.; Charushnikova, I. A.; Krot, N. N.; Yanovskii, A. I.; Struchkov, Y. T. *Radiokhimiya* **1993**, *35*, 24.

(50) Sullivan, J. C.; Hindman, J. C.; Zielen, A. J. *J. Am. Chem. Soc.* **1961**, *83*, 3373.

(51) Sullivan, J. C. *J. Am. Chem. Soc.* **1962**, *84*, 4256.

(52) Sullivan, J. C. *Inorg. Chem.* **1964**, *3*, 315.

(53) Burns, J. H.; Musikas, C. *Inorg. Chem.* **1977**, *16*, 1619.

(54) Siegel, S.; Viste, A.; Hoekstra, H.; Tani, B. *Acta Crystallogr., Sect. B: Struct. Sci.* **1972**, *B28*, 117.

(55) Siegel, S.; Hoekstra, H.; Sherry, E. *Acta Crystallogr.* **1966**, *20*, 292.

(56) Taylor, J. C.; Wilson, P. W. *Acta Crystallogr., Sect. B: Struct. Sci.* **1973**, *B29*, 1073.

(57) Rose, D.; Chang, Y.-D.; Chen, Q.; Zubieta, J. *Inorg. Chem.* **1994**, *33*, 5167.

(58) Ekstrom, A.; Loeh, H.; Randall, C. H.; Szego, L.; Taylor, J. C. *Inorg. Nucl. Chem. Lett.* **1978**, *14*, 301.

(59) Allen, P. G.; Bucher, J. J.; Clark, D. L.; Edelstein, N. M.; Ekberg, S. A.; Gohdes, J. W.; Hudson, E. A.; Kaltsoyannis, N.; Lukens, W. W.; Neu, M. P.; Palmer, P. D.; Reich, T.; Shuh, D. K.; Tait, C. D.; Zwick, B. D. *Inorg. Chem.* **1995**, *34*, 4797–4807.

(60) Jones, L. H. *Spectrochim. Acta* **1958**, *10*, 395.

(61) Jones, L. H. *Spectrochim. Acta* **1959**, *11*, 409.

(62) Nakamoto, K. *Infrared and Raman Spectra of Inorganic Coordination Compounds*, 5th ed.; John Wiley & Sons: New York, 1997; Part A.

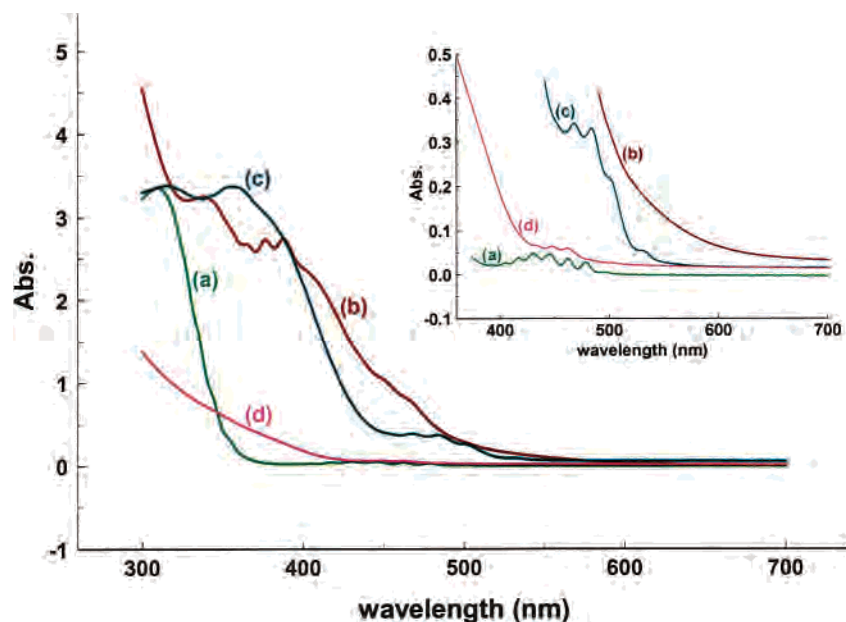


Figure 5. Electronic absorption spectra of (a) $[\text{UO}_2\text{Cl}_2(\text{thf})_3]$ in thf, (b) **2** in toluene, (c) **3** in toluene, and (d) **5** in dichloromethane. The inset shows an expanded version of the region 350–700 nm (all solutions normalized to 11.5×10^{-4} M).

($\nu_1 = 834, 824,$ and 803 cm^{-1} , respectively, for solid-state Raman spectroscopy). The bending of the uranyl unit in **1** can be attributed to a combined effect of weakened $\text{U}=\text{O}$ bonds together with sterically demanding NCN ligands situated on the same side of the uranium pushing the oxo groups away. A similar situation is evident in the only other uranyl complex with a substantial bend (with reliable crystallographic data), $[\text{cis-UO}_2(2,6\text{-}^i\text{BuC}_6\text{H}_3\text{O})_2(\text{thf})_2]$ ($\text{O}=\text{U}=\text{O} = 167.8(4)^\circ$; $\nu_1 = 803 \text{ cm}^{-1}$).⁶³ (The report of an $\text{O}=\text{U}=\text{O}$ angle of 161° for $[\text{UO}_2(\text{ClO}_4)_2] \cdot 10 \cdot 5\text{H}_2\text{O}$ ⁶⁴ was recently proved to be incorrect.⁶⁵) The reduction in ν_1 probably reflects the amount of electron donation to the metal center rather than bending of the uranyl, because the phenyl analogue $[\text{trans-UO}_2(2,6\text{-PhC}_6\text{H}_3\text{O})_2(\text{thf})_2]$ contains a linear uranyl with a similar symmetric stretch ($\text{O}=\text{U}=\text{O} = 178.4(6)^\circ$; $\nu_1 = 808 \text{ cm}^{-1}$).⁶³

Addition of another NCN ligand and replacement of thf on going from **1** to **4** result in a decrease of ν_1 by 30 cm^{-1} to 773 cm^{-1} . A similar but not so dramatic trend is observed in the series of compounds $[\text{UO}_2\text{L}_2\{\text{N}(\text{SiMe}_3)_2\}_2]$, $[\text{Na}(\text{thf})_2][\text{UO}_2\{\text{N}(\text{SiMe}_3)_2\}_3]$, and $[\text{Na}(\text{thf})_2][\text{UO}_2\{\text{N}(\text{SiMe}_3)_2\}_4]$,^{5,38,66} with a decrease in ν_1 ($819, 805,$ and 801 cm^{-1} , respectively) as the number of $[\text{N}(\text{SiMe}_3)_2]^-$ ligands coordinated (2–4) is increased. When the tris adduct $[\text{Na}(\text{thf})_2][\text{UO}_2\{\text{N}(\text{SiMe}_3)_2\}_3]$ and **4** are compared, it is difficult to assign the greater reduction in stretching frequency for **4** to either the greater electron-donating ability of the NCN ligand or out-of-plane distortions in **4**, although we favor the former.

Complex **6** has the second lowest $\text{O}=\text{U}^{\text{VI}}=\text{O}$ ν_1 stretch (757 cm^{-1}) reported for uranyl complexes to date. The only other compound with a lower stretching frequency of 713

cm^{-1} is the tetramer $[\text{UO}_2(\text{OCH}^i\text{Pr})_2]_4$, which contains bridging $\text{UO}_2^{2+} \cdots \text{UO}_2^{2+}$ metal–oxo ligand interactions. A recent study of alkali-metal-encapsulated crown ether complexes of $[\text{UO}_2\text{X}_4]^{2-}$ ($\text{X} = \text{Cl}, \text{Br}$) shows that alkali-metal coordination to the oxo ligands reduces ν_1 by no more than $\sim 10 \text{ cm}^{-1}$.²⁰ By encapsulating Na^+ in 18-crown-6 in **5**, the $\text{O}=\text{U}=\text{O}$ ν_1 stretch increases (785 cm^{-1}) compared to that in **4** (773 cm^{-1}) by $12 \pm 2 \text{ cm}^{-1}$, presumably because of a weaker $\text{U}=\text{O} \cdots \text{Na}$ interaction. Replacing a thf for a NCN ligand (from **1** to **4**) reduces ν_1 by $\sim 30 \text{ cm}^{-1}$, while replacing a thf for a $\mu_2\text{-O}$ (from **1** to **6**) reduces ν_1 by $\sim 50 \text{ cm}^{-1}$. The enhanced ability of the oxide to lower ν_1 may in fact reflect its capacity for effectively competing with the oxo ligands for π -overlap with the 5f and 6d orbitals involved in the uranyl bonding molecular orbitals.⁶⁷ Such a mechanism was suggested to explain the reduced ν_1 (784 cm^{-1}) observed for the tetrahydroxo uranyl complex $[\text{Co}(\text{NH}_3)_6][\text{UO}_2(\text{OH})_4]$ compared to the pentaquo complex $[\text{UO}_2(\text{H}_2\text{O})_5]^{2+}$ ($\nu_1 = 870 \text{ cm}^{-1}$).¹⁴

Electronic Spectroscopy. The electronic transitions of the uranyl ion are complex, with 14 out of 16 possible states identified at low temperature (4.2 K) for the HOMO (σ_u)–LUMO (δ_u/ϕ_u) excitations.^{67–70} At room temperature the absorption spectra for uranyl complexes are generally observed as partially resolved broad bands centered around 400–450 nm containing vibronic fine structure with extinction coefficients of $\sim 10\text{--}50 \text{ dm}^3 \text{ mol}^{-1} \text{ cm}^{-1}$.^{71,72} For example, thf solutions of the bright yellow $[\text{UO}_2\text{Cl}_2(\text{thf})_3]$

(67) Denning, R. G. *Struct. Bonding (Berlin)* **1992**, *79*, 215.

(68) Zhang, Z.; Pitzer, R. M. *J. Phys. Chem. A* **1999**, *103*, 6880.

(69) Matsika, S.; Zhang, Z.; Brozell, S. R.; Blaudeau, J.-P.; Wang, Q.; Pitzer, R. M. *J. Chem. Phys.* **2001**, *105*, 3825.

(70) Denning, R. G.; Snellgrove, T. R.; Woodwark, D. R. *Mol. Phys.* **1976**, *32*, 419.

(71) Rabinowitch, E.; Belford, R. L. *Spectroscopy and Photochemistry of Uranyl Compounds*; Pergamon: London, 1964; Vol. 1.

(72) Ryan, J. L. In *Lanthanides and Actinides*; Bagnall, K. W., Ed.; Butterworth: London, 1972; Vol. 7, pp 323–367.

(63) Wilkerson, M. P.; Burns, C. J.; Morris, D. E.; Paine, R. T.; Scott, B. L. *Inorg. Chem.* **2002**, *41*, 3110–3120.

(64) Alcock, N. W.; Esperás, S. J. *Chem. Soc., Dalton Trans.* **1977**, 893.

(65) Fischer, A. Z. *Anorg. Allg. Chem.* **2003**, *629*, 1012.

(66) Burns, C. J.; Smith, D. C.; Sattelberger, A. P.; Gray, H. B. *Inorg. Chem.* **1992**, *31*, 3724–3727.

show a weak band with fine structure centered at 429 nm ($\epsilon = 38 \text{ dm}^3 \text{ mol}^{-1} \text{ cm}^{-1}$) with a ligand-to-metal charge-transfer (LMCT) band at 320 nm (Figure 5a). This LMCT band is known to move to lower energy with a more reducing ligand, as seen in the series of complexes $[\text{UO}_2\text{X}_2(\text{Ph}_3\text{PO})_2]$ and $[\text{UO}_2\text{X}_4]^{2-}$ (LMCT λ_{max} ; $\text{X} = \text{Cl} < \text{Br} < \text{I}$).⁷³ The most striking features of molecules **1–3** are the colors and the intensities of the colors in solution. These compounds are deep orange in contrast to the normal yellow to yellow/green observed for most uranyl solutions. Despite the fact that there are many uranyl complexes with colors other than yellow reported in the literature, there remains little explanation as to why. Most orange or red uranyl complexes contain strongly electron-donating ligands in the equatorial plane.^{5,10,11,15–17,19,21,38,63,66,74} The argument of λ_{max} being related to LMCT events, and thus the reducibility of the ligand, does not hold true for the red alkoxide $[\text{UO}_2(\text{OCH}(\text{iPr})_2)_4]$ ¹⁶ and aryloxide $[\text{UO}_2(\text{O}-2,6\text{-}^1\text{Bu}_2\text{C}_6\text{H}_3)(\text{thf})_2]$ ⁶³ complexes compared to the orange $[\text{UO}_2\{\text{N}(\text{SiMe}_3)_2\}_2(\text{thf})_2]$.

The electronic absorption spectrum of **1** is very similar to that of **3**. We believe that the equilibrium between **1** and **2** is shifted towards **2** in the very dilute solutions required for UV/vis measurements. Indeed, addition of thf to dilute samples of **2** in toluene changes the band shapes but not their positions. The electronic absorption spectra for **2**, **3** and **5** in the UV/vis region are shown in Figure 5. Compared to $[\text{UO}_2\text{Cl}_2(\text{thf})_3]$, which is considered typical for uranyl complexes, solutions of **2** in toluene exhibit a poorly resolved shoulder at 449 nm ($\epsilon = 921 \text{ dm}^3 \text{ mol}^{-1} \text{ cm}^{-1}$) beneath a very intense structured band at 388 nm ($\epsilon = 2435 \text{ dm}^3 \text{ mol}^{-1} \text{ cm}^{-1}$) and a further strong band at 345 nm ($\epsilon = 3043 \text{ dm}^3 \text{ mol}^{-1} \text{ cm}^{-1}$) (Figure 5b). For toluene solutions of **3** there is a more intense structured band red shifted to 483 nm ($\epsilon = 373 \text{ dm}^3 \text{ mol}^{-1} \text{ cm}^{-1}$) and a second broad signal with overlapping bands at 357 nm ($\epsilon = 3523 \text{ dm}^3 \text{ mol}^{-1} \text{ cm}^{-1}$) (Figure 5c). At first inspection, the intense colors of these solutions are attributed to the strong tail of LMCT bands. On closer inspection the structured band at 388 nm for **2** (Figure 5b) contains progressions $\sim 750 \text{ cm}^{-1}$ apart (relating to the stretching vibration of the uranyl excited state), similar to the separations observed in the vibronic structure of $\sigma_u - \delta_u/\phi_u$ excitation. Progressions can also be identified for $[\text{UO}_2\text{Cl}_2(\text{thf})_3]$ (776 cm^{-1}), **3** (729 cm^{-1}), and **5** (726 cm^{-1}) (Figure 5a,c,d; see inset). In contrast to **1–3** and **5**, complex **4** is not stable in solution and dissociates to give a mixture of $\text{Na}[\text{NCN}]$, **1**, and **4** (by ^1H NMR). The addition of 18-crown-6 to solutions of **4** cleanly generates **5**, demonstrating the increased complexing ability of the ligand when deliberately separated from Na^+ . The UV/vis spectrum of **5** shows a blue shift of the charge-transfer bands compared to those of solutions of **2** and **3** (Figure 5d). A blue shift in absorption

bands is predicted for an increase in coordination number, stronger ligand–ligand repulsions, and increased U–N bond lengths.⁷⁵

Conclusions

We have synthesized and structurally characterized a number of uranyl complexes with sterically demanding ligands that give nontypical coordination geometries. By controlling the coordination number around uranium, it is possible to compare distorted geometries (**1** and **3**) with classical geometries (**2**). The original hypothesis that out-of-plane equatorial ligand coordination causes disruptions to the $\text{O}=\text{U}=\text{O}$ bonding and electronic structure is incorrect. Significant weakening of the uranyl bonding and alteration of the electronic absorption spectrum is achieved using NCN and NPN ligands, but not as a result of geometric distortions. Instead, it is the electron-donating ability of the ligands and their ability to participate in LMCT electronic transitions. Uranyl bond weakening is explained by increased charge at the metal destabilizing the HOMO σ_u orbital, integral to the strength of the uranyl bond.⁶⁷ Coordination of the uranyl oxygens to sodium ions (**4–6**) only facilitates this mechanism. In complex **6**, the combination of strong electron donors ($\mu_2\text{-O}^{2-}$ and NCN ligands) and $\text{U}=\text{O}\cdots\text{Na}$ interactions results in the second lowest reported symmetric stretching frequency for a uranyl(VI) complex (756 cm^{-1}). The electronic transitions are more difficult to rationalize because compound **5** has a low vibrational frequency but no strong LMCT bands above 350 nm. Unfortunately, we have no crystallographic data on **5** to rationalize why this is the case. While there are many examples of uranyl complexes with colors that are red shifted from the more common yellow/yellow-green, no explanation for this is given, although strong donor ligands appear to be involved in most cases. We are endeavoring to investigate this point further.

Experimental Section

General Procedures. Sodium bistrimethylsilylamide (BDH), benzonitrile (anhydrous 99%, Aldrich), was used as received. The compounds $\text{Na}[\text{NPN}]$ ⁷⁶ and $\text{Na}[\text{NCN}]$ ⁷⁷ were synthesized according to the literature; the ligand precursor $(\text{SiMe}_3\text{N})\text{PPh}_2((\text{SiMe}_3)\text{NH})$ was made by refluxing Ph_2PH with 2.5 equiv of SiMe_3N_3 .⁷⁸ The preparation of compound **2** is described elsewhere.²¹ All reactions and manipulations were performed under argon using standard Schlenk techniques or an inert atmosphere drybox. Solvents were purified by distillation from sodium (toluene, hexane), sodium/benzophenone ketyl (thf), and P_2O_5 (CH_2Cl_2) and stored in a drybox. ^1H , $^{13}\text{C}\{^1\text{H}\}$, and $^{31}\text{P}\{^1\text{H}\}$ NMR spectra were recorded on a Bruker Avance 400 instrument at 400, 100, and 162 MHz, respectively. Raman and UV/vis spectroscopy were recorded on Bruker Equinox 55 FTIR/Raman and Varian Cary 500 instruments, respectively. Luminescence measurements were made on a Perkin-Elmer LS 55. Elemental analysis was performed on a Carlo ERBA Instruments

(75) Lever, A. B. P. In *Inorganic Electronic Spectroscopy*; Lever, A. B. P., Ed.; Elsevier: Oxford, 1984; p 203.

(76) Steiner, A.; Stake, D. *Inorg. Chem.* **1993**, *32*, 1977.

(77) Stalke, D.; Wedler, M.; Edelmann, F. T. *J. Organomet. Chem.* **1992**, *431*, Cl.

(78) Paciorek, K. L.; Kratzer, R. H. *J. Org. Chem.* **1966**, *31*, 2426.

(73) Day, J. P.; Venanzi, L. M. *J. Chem. Soc. A* **1966**, 1363.

(74) May, I.; Taylor, R. J.; Denniss, I. S.; Brown, G.; Wallwork, A. L.; Hill, N. J.; Rawson, J. M.; Less, R. *J. Alloys Compd.* **1998**, *275–277*, 769.

CHNS-O EA1108 elemental analyzer for C, H, and N and by a Fisons Horizon Elemental Analysis ICP–OED spectrometer for U and P.

[UO₂(NCN)₂(thf)] (1). A solution of [UO₂Cl₂(thf)₂]₂ (0.500 g, 1.03 mmol) in thf (50 cm³) was treated with a thf (20 cm³) solution of Na[NCN] (1.32 g, 4.12 mmol) and stirred at ambient temperature for 30 min. The resulting bright orange solution was evaporated under vacuum and the residue extracted with hexane (30 cm³). Concentration of the extract, under vacuum, to approximately 15 cm³ and maintaining the temperature at –5 °C for 3 d gave bright orange crystals of **1**·½hexane. Yield: 0.81 g, 43%. ¹H NMR (400 MHz, C₆D₆, 25 °C): δ 0.38 (s, 36H, Si(CH₃)₃), 0.92 (t, 3H, CH₃-hexane), 1.27 (br m, 4H, CH₂-hexane), 1.68 (m, 4H, thf), 4.49 (br m, 4H, thf), 7.17 (m, 6H, *o,p*-Ph), 7.72 (m, 4H, *m*-Ph). ¹³C NMR (100.6 MHz, C₆D₆): δ 3.4 (Si(CH₃)₃), 14.5 (CH₃, hexane), 23.2 (CH₂, hexane), 26.5 (thf), 32.1 (CH₂, hexane), 73.1 (thf), 128.4 (*m*-Ph), 128.9 (*o*-Ph), 129.4 (*p*-Ph), 146.0 (*i*-Ph), 176.8 (NCN). ²⁹Si NMR (79.5 MHz, C₆D₆): δ –0.5. Raman (solid in glass capillary) (cm⁻¹): 3061(s), 2956(s), 2898(vs), 1600(m), 1450(w), 1409(m), 1161(w), 1002(m), 987(w), 803(s), 682(w), 633(m), 403(w). Anal. Calcd for **1**·½hexane C₃₃H₆₁N₄O₃Si₄U: C, 43.45; H, 6.74; N, 6.14. Found: C, 43.79; H, 6.47; N, 6.16.

[UO₂(NPN)₂] (3). A solution of [UO₂Cl₂(thf)₂]₂ (0.250 g, 0.515 mmol) in thf (50 cm³) was treated with a thf (20 cm³) solution of Na[NPN] (0.787 g, 2.06 mmol) and stirred at ambient temperature for 1 h. The resulting bright orange solution was evaporated under vacuum and the residue extracted with hexane (50 cm³). Concentration of the extract, under vacuum, to approximately 25 cm³ and maintaining the temperature at –5 °C for 3 d gave bright orange crystals of **3**. Yield: 0.680 g, 67%. ¹H NMR (400 MHz, C₆D₆, 25 °C): δ 0.27 (s, 36H, Si(CH₃)₃), 7.08 (m, 6H, *o,p*-Ph), 8.25 (m, 4H, *m*-Ph). ³¹P{¹H} NMR (162.0 MHz, C₆D₆): δ 14.6. ¹³C{¹H} NMR (100.6 MHz, C₆D₆): δ 4.0 (d, *J*_{CP} = 3.8 Hz, Si(CH₃)₃), 128.4 (d, *J*_{CP} = 14 Hz, *o*-Ph), 131.4 (d, *J*_{CP} = 2 Hz, *p*-Ph), 133.2 (d, *J*_{CP} = 11 Hz, *m*-Ph), 136.5 (d, *J*_{CP} = 104 Hz, *i*-Ph). ²⁹Si NMR (79.5 MHz, C₆D₆): δ –4.0 (d, *J*_{SiP} = 5.6 Hz). Raman (solid in glass capillary) (cm⁻¹): 3060(s), 2955(s), 2898(vs), 1592(m), 1400-(br w), 1181(w), 1110(w), 1028(w), 1000(s), 824(s), 668(w), 622-(m). Anal. Calcd for **3**, C₃₆H₅₆N₄O₂P₂Si₄U: C, 43.71; H, 5.71; N, 5.66; P, 6.27, U, 24.06. Found: C, 43.44; H, 5.65; N, 5.55; P, 5.91; U, 23.36.

[Na(thf)₂(PhCN)_{0.5}][UO₂(NCN)₃] (4·½PhCN). A solution of [UO₂Cl₂(thf)₂]₂ (0.50 g, 1.03 mmol) in thf (50 cm³) was treated with a thf (20 cm³) solution of Na[NCN] (1.98 g, 6.18 mmol) and stirred at ambient temperature for 30 min. The resulting bright orange solution was evaporated under vacuum and the residue extracted with hexane (2 × 50 cm³). Concentration of the extract, under vacuum, to approximately 50 cm³ and maintaining the temperature at –5 °C for 1 d gave bright orange crystals of **4**·

½PhCN that lose PhCN upon drying under vacuum. Yield: 1.96 g, 74%. ¹H NMR (400 MHz, C₆D₆, 25 °C): δ (major species in solution) 0.34 (s, 54H, Si(CH₃)₃), 1.44 (br m, 8H, CH₂-thf), 3.801 (br, 8H, CH₂O-thf), 6.64 (m, 1H, *o*-PhCN), 6.81 (m, 1H, *m*-PhCN), 7.01–7.17 (m, 12H, *o,m*-Ph) 7.72 (d, 3H, *J* = 7 Hz, *p*-Ph), 7.79 (d, 0.5H, *J* = 7 Hz, *p*-PhCN). ¹³C NMR (100.6 MHz, C₆D₆): δ 3.0 (Si(CH₃)₃), 25.8 (thf), 69.7 (thf), 111.6 (*o*-PhCN), 119.7 (*m*-PhCN), 127.4 (*p*-PhCN), 128.4 (*m*-Ph), 128.9 (*o*-Ph), 129.4 (*p*-Ph), 145.9 (*i*-Ph), 147.0 (*i*-PhCN), 175.9 (PhCN), 177.3 (NCN). Raman (solid in glass capillary) (cm⁻¹): 3061(s), 2954(vs), 2896-(vs), 1600(m), 1409(m), 1251(w), 1164(m), 1030(w), 1002(s), 987-(w), 773(s), 689(w), 633(m), 606(w), 484(w), 383(w). Anal. Calcd for **4**, C₄₇H₈₅N₆NaO₄Si₆U: C, 45.98; H, 6.98; N, 6.84; Na, 1.87; U, 19.39. Found: C, 45.05; H, 6.82; N, 7.19; Na, 2.32; U, 19.12.

[Na(18-crown-6)][UO₂(NCN)₃] (5). A solution of **4** (0.348 g, 0.283 mmol) in diethyl ether (10 cm³) was treated with a diethyl ether solution of 18-crown-6 (0.015 g, 0.566 mmol). A bright yellow solid that precipitated immediately was washed with diethyl ether (2 × 10 cm³) and dried under vacuum to give bright yellow microcrystalline **5**. Yield: 0.377 g, 99%. ¹H NMR (400 MHz, CD₂-Cl₂, 25 °C): δ 0.01 (s, 54H, Si(CH₃)₃), 3.62 (s, 24H, 18-crown-6), 7.30 (m, 3H, *p*-Ph) 7.34 (m, 6H, *o*-Ph), 7.65 (m, 6H, *o*-Ph). ¹³C NMR (100.6 MHz, CD₂-Cl₂): δ 3.8 (Si(CH₃)₃), 69.5 (18-crown-6), 126.8 (*p*-Ph), 127.1 (*o*-Ph), 128.9 (*m*-Ph), 149.0 (*i*-Ph), 174.6 (NCN). Raman (solid in glass capillary) (cm⁻¹): 3062(vs), 2954-(vs), 2895(vs), 1600(s), 1448(w), 1410(m), 1276(w), 1247(w), 1165-(m), 1030(w), 1001(s), 988(w), 866(w), 834(w), 785(s), 703(w), 685(w), 630(s), 486(w), 394(w), 326(w). Anal. Calcd for **5**, C₅₁H₉₃N₆NaO₈Si₆U: C, 45.45; H, 6.95; N, 6.24; U, 17.66. Found: C, 44.38; H, 6.64; N, 6.23; U, 17.69.

[Na(thf)UO₂(NCN)₂]₂(μ-O) (6). This compound was formed as a minor product in the synthesis of **4**. Only single-crystal X-ray diffraction and Raman spectroscopy data were measured on the small amount of sample obtained. Raman (solid in glass capillary) (cm⁻¹): 3060(vs), 2951(vs), 2894(vs), 1600(s), 1408(m), 1249-(w), 1160(m), 1029(w), 1001(s), 984(s), 757(s), 701(m), 633(m), 616(w), 487(w), 401(w).

Acknowledgment. We thank Dr. David Collison and Dr. Iain May of The University of Manchester for helpful discussions and BNFL for the financial support via an Industrial Fellowship (M.J.S.).

Supporting Information Available: Crystallographic files for compounds **2**, **3**, **4** and **6** (CIF), solution and solid-state Raman spectra, variable-temperature NMR spectra of **2**, and UV/vis spectra of ligand salts Na[I] and Na[II]. This material is available free of charge via the Internet at <http://pubs.acs.org>.

IC035349C